Research Article

Soret–Dufour and radiative aspects in hydromagnetized nanofluid flow in stratified porous medium

M. I. Anwar[1,2,3] · M. Ali[4] · K. Rafique[3] · S. A. Shehzad[5]

Abstract
The numerical computations of Soret–Dufour aspects in hydromagnetics nanofluid flow in thermal stratified porous medium under radiated chemical reaction are developed. The unique similarity transformations lead to reduce the partial differential system into expressions of ordinary ones. Keller-box approach is adopted to express the numeric solutions. The impacts of embedded flow parameters on the different flow profiles signifying velocity, concentration and temperature of nanofluid are discussed via graphs. The values of $-\theta'(0)$, $-\phi'(0)$ and $-f''(0)$ in relation with the variation in sundry physical parameters are examined through numerical benchmarks. The numerical results in special cases agreed with published work showing the validity of formulated problem. It can be seen that the temperature profile enhances for cumulative values of Brownian motion and thermophoretic impacts. In addition, the enhancement in Dufour factor declines the temperature profile. On contrast, larger the Soret parameter results an increase in concentration profile. On the other hand, chemical reaction shows direct relation with temperature profile.

Keywords Radiation effect · Chemical reaction · Thermal stratification · Soret–Dufour effects · Stratified medium

1 Introduction

Soret–Dufour aspects in the heat transportation problems are of enormous curiosity and widely growing interest in such type of investigations becomes on peak due to emerging implications in disticnt branches such as geosciences, chemical engineering, hydrology and petrology. Various flow analysis have been performed on these effects encountered in number of processes by means of different interesting experimental and theoretical methodologies. The creation of fluxes associated with heat-mass transfer is well-known phenomenon, the mass flux in result of temperature gradient is familiar as Soret effect. Also, Dufour effect which is the generation of energy flux from concentration gradients. These effects are second ordered phenomena that are reciprocal processes. Sometimes these ignored and neglected in different flow problems because of very smaller order of magnitudes on comparing with Fick's and Fourier's laws aspects. According to Eckert and Drake [1], these cannot be ignored in many cases like in separation of isotope and fluids of medium molecular weight. Soret–Dufour in mass heat flow phenomenon was carried out by Chapmanand and Cowling [2] by employing the gases kinetic theory. Furthermore, the Soret–Dufour effects in monatomic polyatomic/gases mixtures was developed by Hirshfelder et al. [3]. In addition, flow through porous media is engaged for different purpose like as filtration and purification, the water resources underground the earth surface, disposal of nuclear wastes in the soil. In petroleum industries, these are utilized to examine the motion of natural gas, water and oil in the oil reservoirs and also used to enhance the oil recovery. With

✉ S. A. Shehzad, ali_qau70@yahoo.com | [1]Department of Mathematics, Faculty of Science, University of Sargodha, Sargodha, Pakistan. [2]Higher Education Department (HED), Lahore, Punjab, Pakistan. [3]School of Quantitative Sciences, Universiti Utara Malaysia, 06010 Sintok, Kedah, Malaysia. [4]Department of Mathematics, Ripah International University, Faisalabad Campus, Faisalabad, Pakistan. [5]Department of Mathematics, COMSATS University Islamabad, Sahiwal 57000, Pakistan.

SN Applied Sciences (2019) 1:1430 | https://doi.org/10.1007/s42452-019-1473-5

Received: 20 August 2019 / Accepted: 7 October 2019 / Published online: 17 October 2019

the emerging applications, the researcher's attempts on Soret–Dufour aspects of fluid flow are referred to [4–9].

Stratification is the feature of all liquids that enclosed by differentially heated walls. The effects of thermal stratification can be produced when the thermal boundary layer continuously discharge within the medium. When a hot fluid discharge over a cold region, thermal stratification can be produced with lighter liquid overlying dense liquid. The dynamics of flows owing to a hot surface embedded in a thermally stratified fluid is characterized by the researchers in numerous studies during the last few years. Generally, thermal stratification is encountered in the heat transfer processes of chemical and hydrometallurgical industries. Existing of these effects in flow over stretchable surfaces become most valuable. For instance, during the polymer extrusion, the object pass through a die and then proceed under a suitable temperature for cooling. The rate of cooling has considerable role in the final product having suitable properties. Considering thermal stratification effects, there are pertinent research works [10–13] has been carried out by investigators in this regard.

Choi [14] first time introduced the nanofluid which is special class of fluids and nanotechnology is based on the nanofluid become a large field of research among the researchers during the last few decades. Nanofluids are prepared by the stable and uniform suspensions of nanometer sized solid particles called nanoparticles (Al_2O_3, Cu, CuO) in the liquids. Nanofluid has plenty of important applications in engineering and technology and widely used for thermal processes at industrial level. Choi also described these suspensions of nanoparticles can be used for the enhancement of the thermal conductivity of other fluids because these are unique in thermal, mechanical, optical, electrical and magnetic properties. Further, he pointed out that nanofluid are best candidates for heat and mass transfer when these are compared with the other fluids. For applications of nanofluid, see [15–18].

The model of Tiwari-Das [19] and Buongiorno [20] are used widely for the behavior of nanofluid by different investigators. The Tiwari-Das model is effective especially for volumetric fraction of the nanoparticles in the parent fluids. The characetrization of Brownian and thermophoresis factors is made in Buongiorno model. This model exposed improvement of heat transfer in convective states instead of the thermophysical properties of nanofluids and explained different ways to enhance the thermal conductivity in relation with the parent fluids. It is also pointed out that nanoparticles occupying Brownian motion and thermophoresis impacts cause enhancement of thermal conductivity. Recently, Sheikholeslami, and Rokni [21] considered the non-equilibirium model for the flow of nanofluid through a porous cavity. Moreover, Sheikholeslami et al. [22] used two phase model (Lgrangian-Eulerian approach) for the flow of nanofluid through a wavy chamber. Numerous investigators [23–26] used Buongiorno model to study flow characteristics.

Several researchers explored the MHD effects in numerous energy-related flows induced by stretching sheet. MHD flows are accounted in many processes such as flow meters, MHD power generators, energy recovery, plasma studies, aerodynamic and solar energy devices. The physical effects in MHD offer influential situations in heat flow problems. The Lenz's law indicates that the electric current is induced on a moving conductor under the magnetic field impacts which comprises its own magnetic field. The motion of fluid modifies when conducting fluid moves under the impact of magnetic field, the magnetic nanoparticles interact with Lorentz forces. MHD fluids controlled system performance by means of electrically conducting fluids. For brief knowledge, one can see researcher attempts on MHD effects in references [27–36].

The chemical reaction is stimulus and widely exist in nature and well as in chemical industries. It occupies lot of applications in chemical engineering and useful in ceramics, food processing and polymer productions etc. In addition, a vast variety of situations occurs in technology where high temperature is necessary and impacts of radiation become most valuable. Some processes are power plants for power generation, spacecrafts engines, space exploration, hypersonic light and solar power devices. In view of such important reasons, many researchers [37–40] have been reported various studies in this direction.

The motivation behind the consideration of the current model is the importance of key parameters i.e. Browinan motion and thermophoretic impacts. According to Boungiorno's these impacts are triggered the enhancement of thermal conductivity of the base fluids. In addition, keep in mind the growing need of heat exchange processes in industry and nuclear reactors we develop the current nanofluid study from the Boungiorno model.

2 Problem formulation

Consider the two dimensional coordinate system in a manner that *x*-axis is directed to stretching sheet inserted inside the porous medium and the y-axis is upward direction to sheet. It is assumed that the stretched and free-stream velocities are defined by $u_w(x) = ae^{x/\ell}$ and $u_\infty(x) = 0$, where x is coordinate parallel to sheet, l is denoting length of stretching sheet while $a > 0$ is constant. Also assumed a non-uniform transversely applied magnetic field having the strength $B = B_o e^{x/\ell}$. Also, no external electrical field supposed to exist, so that the impact of polarization of charges is negligibly small [41]. The induced magnetic field created by nanofluid (electrically conducting) motion is also

in negligibly small amount as in comparison with applied one. Flow geometry is illustrated in Fig. 1.

The governing equations in the usual dimensional forms are:

$$\frac{\partial v}{\partial y}+\frac{\partial u}{\partial x}=0, \tag{1}$$

$$v\frac{\partial u}{\partial y}+u\frac{\partial u}{\partial x}=\frac{\mu}{\rho_f}\frac{\partial^2 u}{\partial y^2}-\left(\frac{\nu}{K}+\frac{\sigma B_o^2}{\rho_f}\right)u, \tag{2}$$

$$\begin{aligned} v\frac{\partial T}{\partial y}+u\frac{\partial T}{\partial x}&=\alpha\frac{\partial^2 T}{\partial y^2}-\frac{1}{(\rho c)_f}\frac{\partial q_r}{\partial y}\\ &+\tau\left[\left(\frac{\partial T}{\partial y}\right)^2\frac{D_T}{T_\infty}+D_B\frac{\partial T}{\partial y}\frac{\partial C}{\partial y}\right]+\frac{D_T K_T}{C_s C_{p^*}}\frac{\partial^2 C}{\partial y^2}, \end{aligned} \tag{3}$$

$$v\frac{\partial C}{\partial y}+u\frac{\partial C}{\partial x}=D_B\frac{\partial^2 C}{\partial y^2}-R\left(C-C_\infty\right)+\frac{\partial^2 T}{\partial y^2}\frac{D_T K_T}{T_\infty}. \tag{4}$$

The symbols used in above expressions are: x and y show the Cartesian coordinates measured directed to the stretching sheet and normal to it while u and v the velocity components in x and y coordinates, ρ_f the density, ν the kinematic viscosity, K the permeability of porous medium, σ the electric conductivity, B_0 the uniform magnetic field, $\alpha=\frac{k}{(\rho c)_f}$ the thermal diffusivity, τ the thermophoretic, D_B the Brownian diffusion, D_T the thermophoretic, K_T the ratio of thermal diffusion, C_S the concentration susceptibility and C_{p^*} the specific heat capacity.

Employing Rosseland approximation (radiation flux) [42] for an optically thick layer one has:

$$q_r=-\frac{4\sigma^*}{3k^*}\frac{\partial T^4}{\partial y}. \tag{5}$$

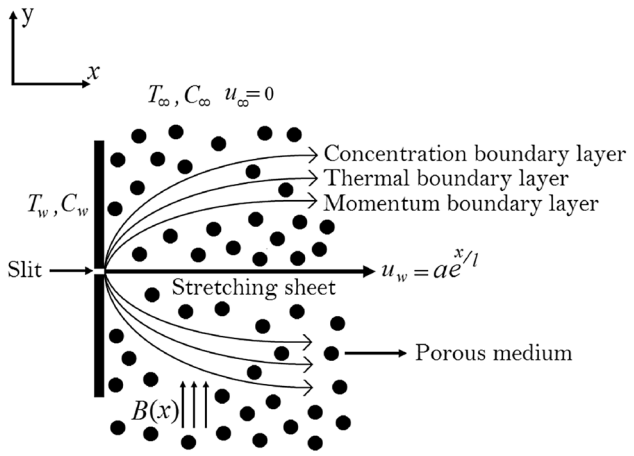

Fig. 1 Flow diagram with coordinates

The term T^4 in radiation flux formula can be solved in Taylor series about T_∞ and when high order expressions eliminate, it gives

$$T^4\cong 4T_\infty^3 T-3T_\infty^4. \tag{6}$$

In the view of expressions (5) and (6), Eq. (3) changes to

$$\begin{aligned} \frac{\partial T}{\partial y}+u\frac{\partial T}{\partial x}&=\left(\alpha+\frac{16\sigma^* T_\infty^3}{3k^*(\rho c)_f}\right)\frac{\partial^2 T}{\partial y^2}\\ &+\tau\left[\left(\frac{\partial T}{\partial y}\right)^2\frac{D_T}{T_\infty}+D_B\frac{\partial T}{\partial y}\frac{\partial C}{\partial y}\right]+\frac{D_T K_T}{C_s C_{p^*}}\frac{\partial^2 C}{\partial y^2}. \end{aligned} \tag{7}$$

The subjected boundary conditions are:

$$\begin{aligned} &u=u_w(x)=ae^{\frac{x}{\ell}},\ v=0,\ C=C_w(x),\ T=T_w(x)\ \text{at}\ y=0,\\ &u\to 0,\ v\to 0,\ C\to C_\infty,\ T\to T_\infty=nT_w(x)+(1-n)T_o,\ \text{as}\ y\to\infty. \end{aligned} \tag{8}$$

where n denotes constant known as thermal stratification parameter which can be taken in the way $0\le n<1$ and equal to $\frac{m_1}{1+m_1}$ where m_1 shows constant. The prescribed temperature and concentration over the stretchable surface can be defined as

$$T_w(x)=T_\infty+T_o e^{x/2\ell}, C_w(x)=C_\infty+C_o e^{x/2\ell} \tag{9}$$

where T_o is the reference temperature while C_o denotes the reference concentration. In order to obtain nonlinear ordinary form of flow equations, An appropriate stream function $\psi=\psi(x,y)$ satisfying continuity Eq. (1) with the similarity transformations are taken as:

$$\begin{aligned} &\psi=\sqrt{2\ell\upsilon a}e^{\frac{x}{\ell}}f(\eta),\ \theta(\eta)(-T_\infty+T_w)=\left(-T_\infty+T\right),\ u=\frac{\partial\psi}{\partial y},\\ &\phi(\eta)\left(-C_\infty+C_w\right)=\left(-C_\infty+C\right),\ \eta=y\sqrt{\frac{a}{2\upsilon\ell}}e^{x/\ell},\ v=-\frac{\partial\psi}{\partial x}, \end{aligned} \tag{10}$$

Equation (2), (4) and (7) reduced with the help of (10) into the following forms:

$$f'''-(K_1+M)f'+ff''-2f'^2=0, \tag{11}$$

$$Pr_N\theta''+Nt\theta'^2+D_f\phi''+f\theta'-f'\theta-\left(\frac{n}{1-n}\right)f'+Nb\theta'\phi'=0, \tag{12}$$

$$\phi''-Le\,f'\phi+Le\,f\phi'-Le\,R\phi+S_r\,Le\,\theta''=0. \tag{13}$$

The derivative of variables with respect to η are indicated by superscript $'$, $Pr=\frac{\nu}{\alpha}$ the Prandtl number, $Le=\frac{\nu}{D_B}$ the Lewis number, $M=\frac{2l\sigma B_o^2}{a\rho_f}$ the Hartmann number, $K_1=\frac{2l\nu}{aKe^{x/\ell}}$ the permeability parameter, $Pr_N=\frac{1}{Pr}\left(1+\frac{4}{3}N\right)$ the modified Prandtl number where $N=\frac{4\sigma^* T_\infty^3}{\alpha k^*(\rho c)_f}$ the radiation constraint, $R=\frac{2lR^*}{u}$ the chemical reaction constraint,

$S_r = \frac{D_T K_T (T_w - T_\infty)}{\nu T_\infty (C_w - C_\infty)}$ the Soret number, $D_f = \frac{D_T K_T (C_w - C_\infty)}{\nu C_s C_{p^*} (T_w - T_\infty)}$ the Dufour number, $Nt = \frac{\tau D_T (T_w - T_\infty)}{\nu T_\infty}$ the thermophoresis parameter and $Nb = \frac{\tau D_B (C_w - C_\infty)}{\nu}$ the Brownian motion constraint. The corresponding boundary conditions (8) become

$$\begin{aligned} &f(\eta) = 0,\ f'(\eta) = 1,\ \phi(\eta) = 1,\ \theta(\eta) = 1 \text{ at } \eta = 0,\\ &f'(\eta) \to 0,\ \phi(\eta) \to 0,\ \theta(\eta) \to 0 \text{ at } \eta \to \infty. \end{aligned} \tag{14}$$

The skin friction, Sherwood number and Nusselt number for the current study are regarded as

$$Nu_x = \frac{x q_w}{k(T_w - T_\infty)},\ Sh_x = \frac{x q_m}{D_B(C_w - C_\infty)},\ C_f = \frac{t_w}{u_w^2 \rho_f} \tag{15}$$

where $q_w = -k\frac{\partial T}{\partial y}, q_m = -D_B\frac{\partial C}{\partial y}, \tau_w = \mu\frac{\partial u}{\partial y}, aty = 0,$

The related terms of dimensionless reduced Nusselt number $-\theta'(0)$, reduced Sherwood number $-\phi'(0)$ and skin friction coefficient C_{fx} are:

$$\begin{aligned} C_{fx}(0) &= C_f\sqrt{\left(\frac{2l}{x}\right)Re_x},\ -\theta'(0)\\ &= \frac{Nu}{\left(1 + \frac{4}{3}N\right)\sqrt{\left(\frac{x}{2l}\right)Re_x}},\ -\phi'(0)\\ &= \frac{Sh}{\sqrt{\left(\frac{x}{2l}\right)Re_x}}. \end{aligned} \tag{16}$$

where $Re_x = \frac{U_w(x)x}{\nu}$ is the local Reynolds number. In order to get a numerical solution of the developed equations, Keller Box method is used an efficient scheme which is best for calculating boundary-layer stream. The equations proceed under the finite difference derivatives, Newton's, block-elimination methods and computed by MATLAB by defining suitable starting conditions. For detailed methodology of this procedure, see [43].

3 Results and discussions

A series of numerical computations has been performed by implementing a useful numerical scheme called the Keller-box method on system of Eqs. (11–13) with their appropriate boundary conditions (14) to obtain an insight into the physical situation of flow configuration. These computations are obtained for numerous magnitudes of Pr, Nb, Nt, M, Le, K_1, S_r, N, R, D_f and n which are displayed in Tables 1 and 2 and graphical format (Figs. 2, 3, 4, 5, 6, 7, 8, 9, 10, 11, 12, 13, 14, 15, 16 and 17). A comparison has been provided among currently acquired results and literature

Table 1 The values of $-\theta'(0)$ for $Nt = Nb = K_1 = D_f = S_r = Le = n = R = 0$

Pr	M	N	$-\theta'(0)$ Bidin and Nazar [44]	$-\theta'(0)$ Present results
1.0	0.0	0.0	0.9548	0.9548
2.0	0.0	0.0	1.4714	1.4714
3.0	0.0	0.0	1.8691	1.8691
1.0	0.0	1.0	0.5315	0.5312
1.0	1.0	0.0	–	0.8611
1.0	1.0	1.0	–	0.4505

results displaying well agreement which verify accuracy of studied problem.

Table 1 gives the accuracy of present investigation by providing agreement for $-\theta'(0)$ with other publications while Table 2 provides the clear insight of $-\theta'(0)$, $-\phi'(0)$ and $C_{fx}(0)$ vary with respect to alteration in values of Nt, Pr, Nb, M, Le, K_1, N, R, D_f, n and S_r in such a way that one parameter increases while all other parameters remain fix at particular values. One can easily noticed that $-\theta'(0)$ shows rise in case of rising values for Nt, Pr, M and K_1 but for higher the values of Le , Nb, N, R , D_f, n and S_r, $-\theta'(0)$ decreases. It is also observed that $-\phi'(0)$ increases when N, R, Nb, D_f, Le, n and S_r enhance but when Nt, Pr, M and K_1 enhance, $-\phi'(0)$ depicts decline. No changes are observed in $C_{fx}(0)$ in case of increment in Nt, Nb, Pr, Le, N, R, D_f, n and S_r while $C_{fx}(0)$rises for M and K_1 only.

Figures 2 and 3 express the velocity profile for numerous values of the parameters characterizing the flow velocity. It is observed that increase of K_1 reduces the velocity profile. It is now a well-established fact that high resistance is offered by porous medium by means of high shear stress opposite to the flow in case of increasing permeability parameter. As a result, velocity profile decreases. Interaction of Lorentz force and flow boost up by enhancing M. Hence, the flow becomes slow and velocity profile reduces, which is illustrated in Fig. 3.

Figures 4, 5, 6, 7, 8, 9, 10 and 11 depict the impacts of different parameters on temperature distribution. It is remarked by Fig. 4 that, a rise in n leads to enhance temperature profile. A reverse trend (decrease) is noticed from temperature profile in case of increasing the values of N as described by Fig. 5. It is clear from Fig. 6 that the temperature profile enhances with the enhancing values of R. Also the temperature contour decreases by growing the magnitudes of Pr expressed by Fig. 7. The contribution of this parameter in the reduction temperature profile is justified as the ratio of viscous diffusion rate to thermal diffusion rate depicts the basic definition of Prandlt number so

Table 2 The calculations of $-\theta'(0)$, $-\phi'(0)$ and $C_{fx}(0)$ with variations

Nb	Nt	Pr	Le	M	K_1	R	N	D_f	S_r	n	$-\theta'(0)$	$-\phi'(0)$	$C_{fx}(0)$
0.1	0.1	7.0	5.0	0.1	1.0	1.0	1.0	0.1	0.1	0.1	1.0026	3.3079	1.4491
0.5	0.1	7.0	5.0	0.1	1.0	1.0	1.0	0.1	0.1	0.1	−0.1682	3.3793	1.4491
0.1	0.3	7.0	5.0	0.1	1.0	1.0	1.0	0.1	0.1	0.1	4.9156	3.0670	1.4491
0.1	0.1	8.0	5.0	0.1	1.0	1.0	1.0	0.1	0.1	0.1	1.4386	2.7411	1.4491
0.1	0.1	7.0	10.0	0.1	1.0	1.0	1.0	0.1	0.1	0.1	0.5647	5.1739	1.4491
0.1	0.1	7.0	5.0	2.5	1.0	1.0	1.0	0.1	0.1	0.1	1.2942	2.7825	2.1213
0.1	0.1	7.0	5.0	0.1	2.0	1.0	1.0	0.1	0.1	0.1	2.2214	3.0666	1.7607
0.1	0.1	7.0	5.0	0.1	1.0	3.0	1.0	0.1	0.1	0.1	0.9046	4.7633	1.4491
0.1	0.1	7.0	5.0	0.1	1.0	1.0	5.0	0.1	0.1	0.1	0.5601	3.3315	1.4491
0.1	0.1	7.0	5.0	0.1	1.0	1.0	1.0	0.3	0.1	0.1	−1.4558	3.8343	1.4491
0.1	0.1	7.0	5.0	0.1	1.0	1.0	1.0	0.1	0.3	0.1	−0.3007	3.6656	1.4491
0.1	0.1	7.0	5.0	0.1	1.0	1.0	1.0	0.1	0.1	0.2	0.4285	3.3468	1.4491

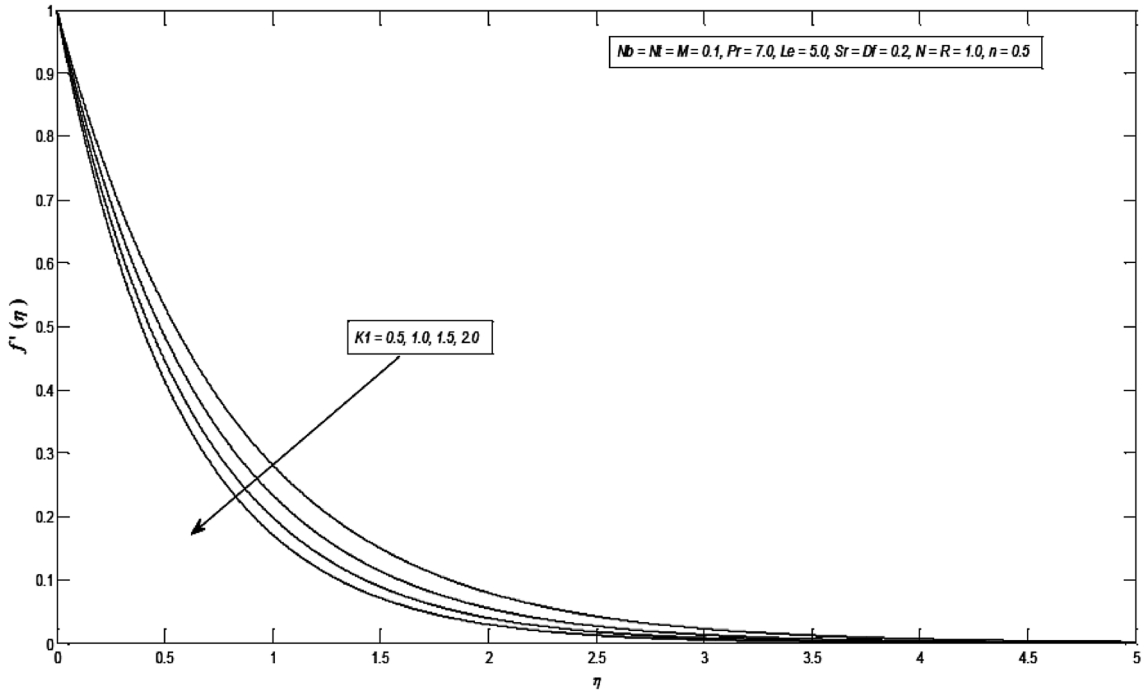

Fig. 2 The impacts of K_1 on $f'(\eta)$

that the enhancement in the size of nanoparticles and the viscosity of the parent fluid leads to enhance this number. In this way, the conduction phenomenon occurs within the flow system and the thermal diffusivity decreases. As a result, heat transfer becomes lower. The Fig. 8 represents that the temperature profile enhances by increasing Nb. This trend is also observed in case of Nt in Fig. 9. This is due to fact that the nanoparticles in the parent fluid collide each other gain kinetic energy and their motions show zig-zagging way. When Nb increases, these zigzag motions of nanoparticle become more rapid and the temperature in the hot regime rises. On the other side, good nanoparticles distributions are related to increment of Nt because thermophoresis effects force particles to move hot to cold area. It is noted from Fig. 10 that, enhancement of M results increase in temperature profile. Since the Lorentz force decline the flow velocity, which is accompanied by rise in temperature. Thus, the magnetic effects heat the fluid. The subsequentrise in D_f reduces the temperature profile as expressed by Fig. 11.

Figures set 12, 13, 14, 15, 16 and 17 display the impacts of the parameters characterizing the concentration distributions. Figure 12 reveals that, the concentration profile enhances by rising the values of S_r. According to Fig. 13,

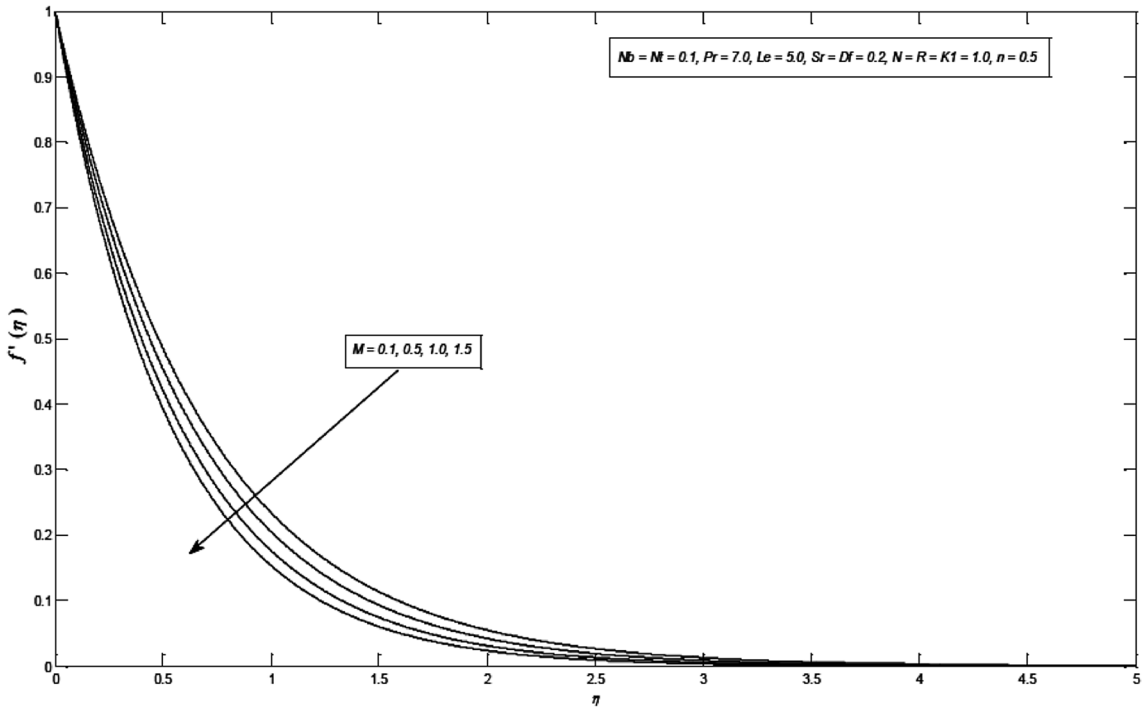

Fig. 3 The impacts of M on $f'(\eta)$

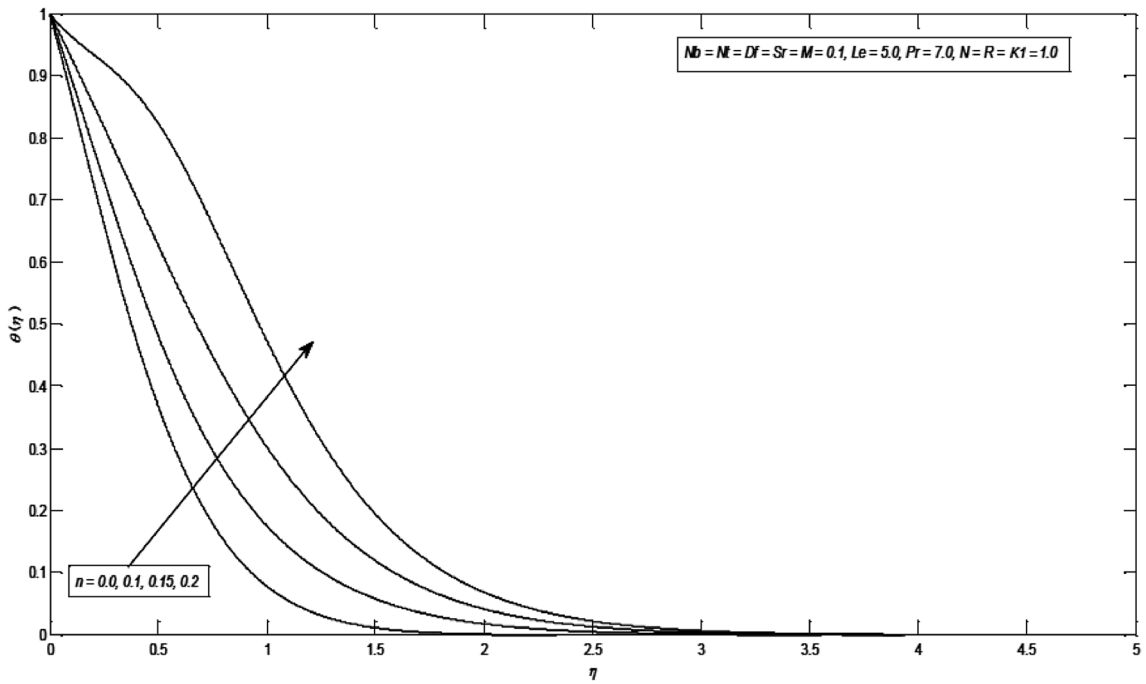

Fig. 4 The impacts of n on $\theta(\eta)$

the concentration profile shows decline by increasing the values of R. This happens due to consumption of chemicals during the flow. The concentration profile becomes smaller in relation with increment of parameter Nb in Fig. 14. It is also clear in Fig. 15 that larger the values of Nt causes enhancement in concentration profile. Figure 16 exhibits that the concentration profile enhances by rising

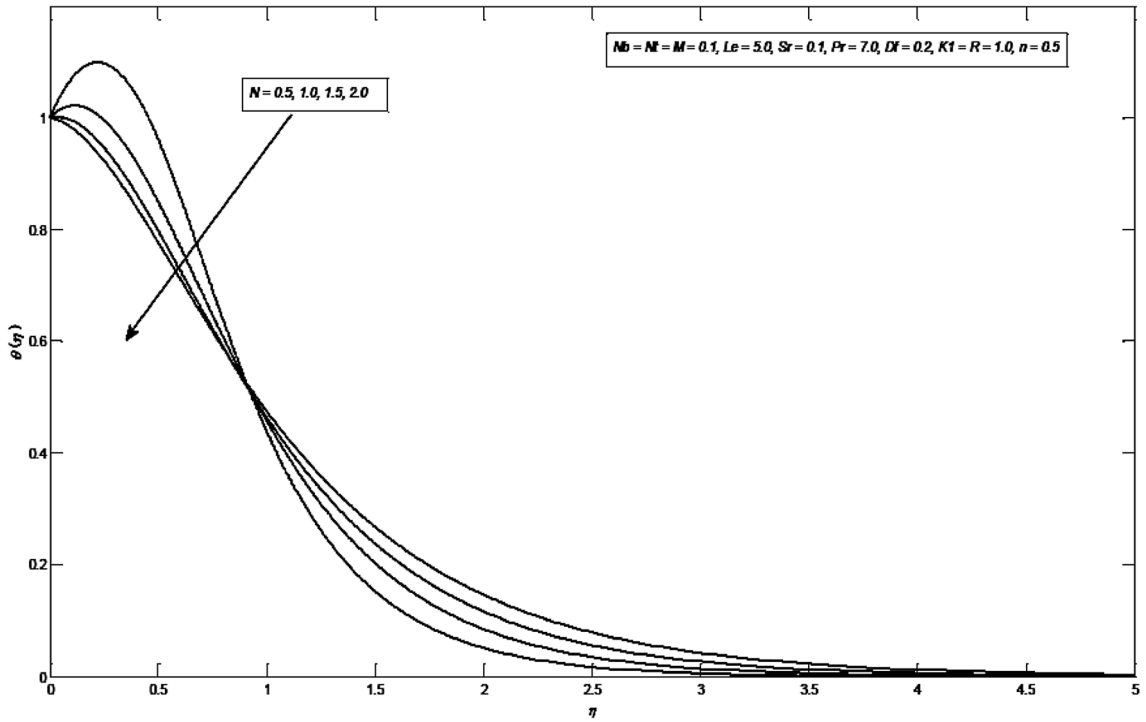

Fig. 5 The impacts of N on $\theta(\eta)$

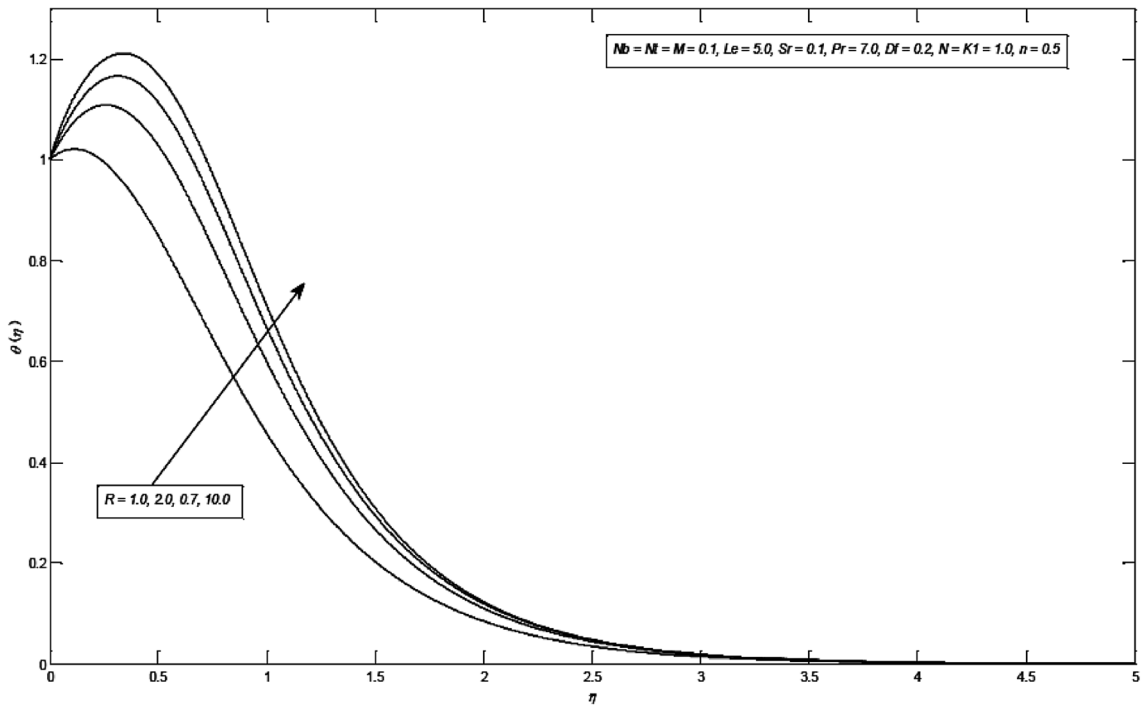

Fig. 6 The impacts of R on $\theta(\eta)$

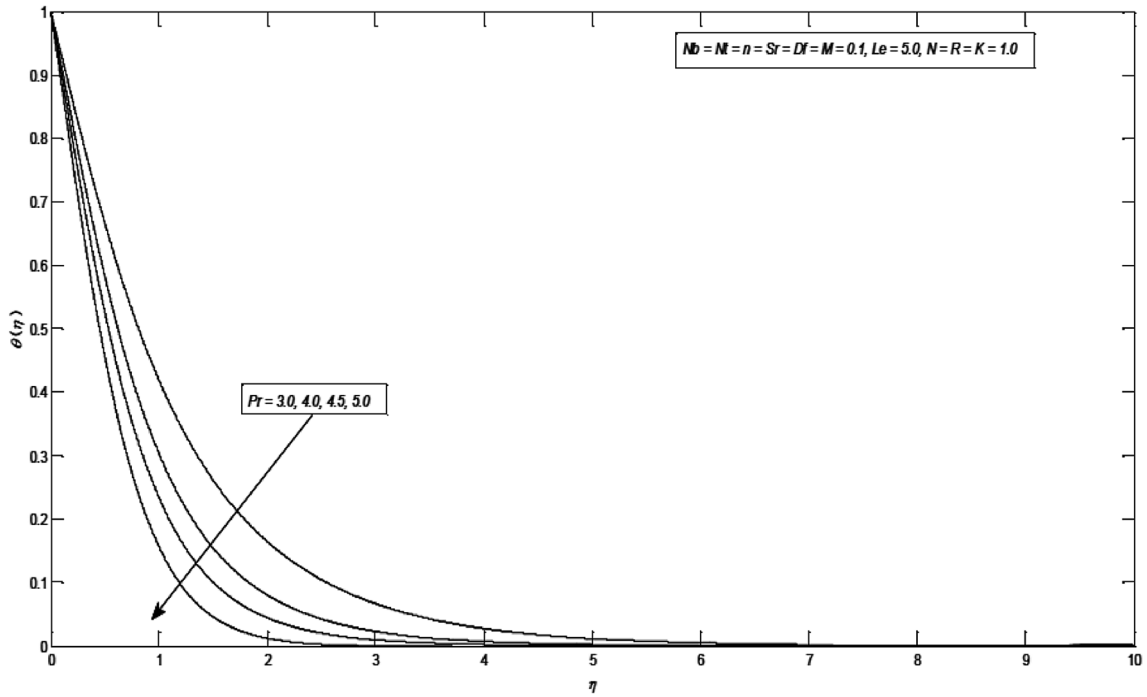

Fig. 7 The impacts of Pr on $\theta(\eta)$

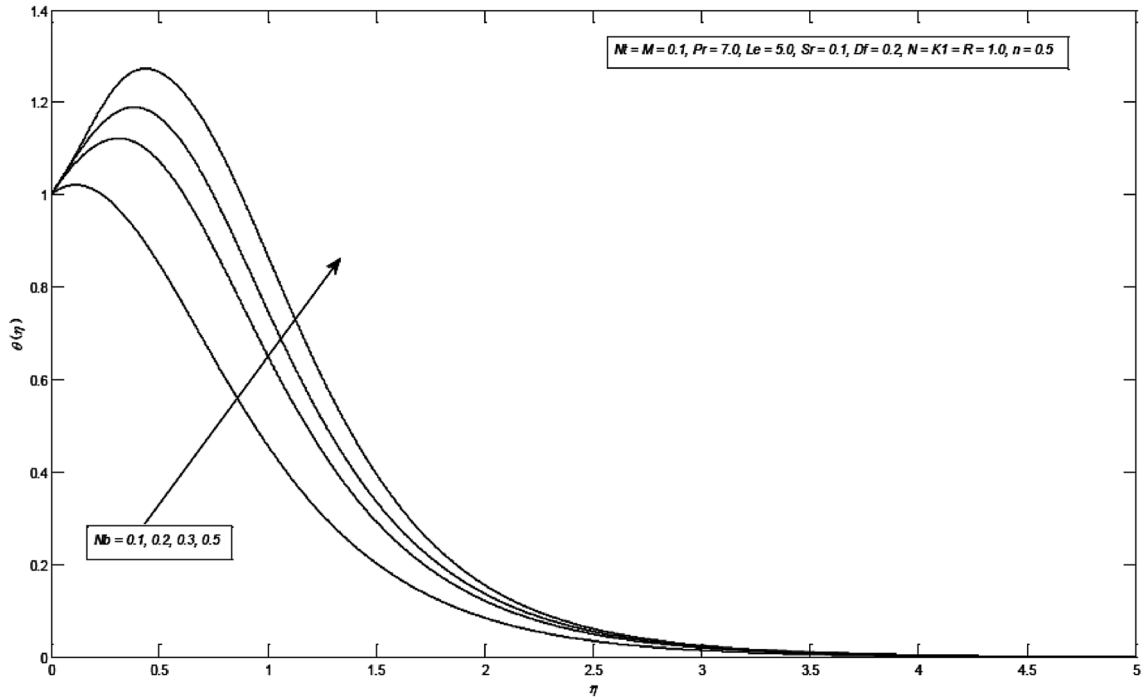

Fig. 8 The impacts of Nb on $\theta(\eta)$

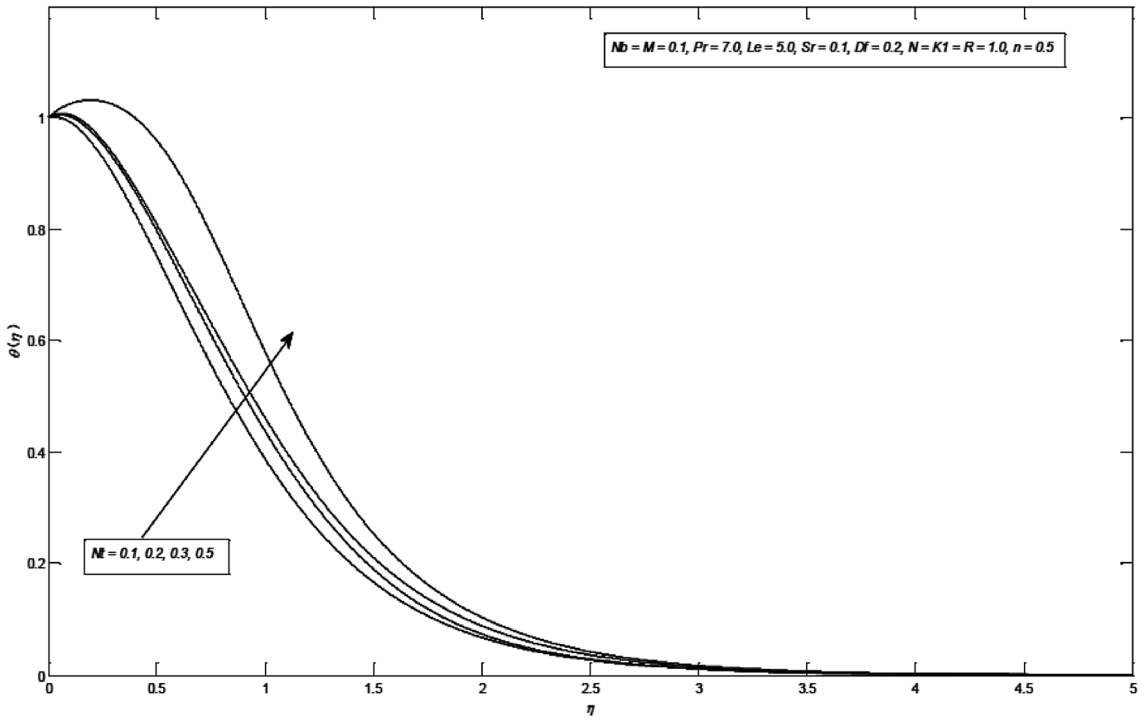

Fig. 9 The impacts of Nt on $\theta(\eta)$

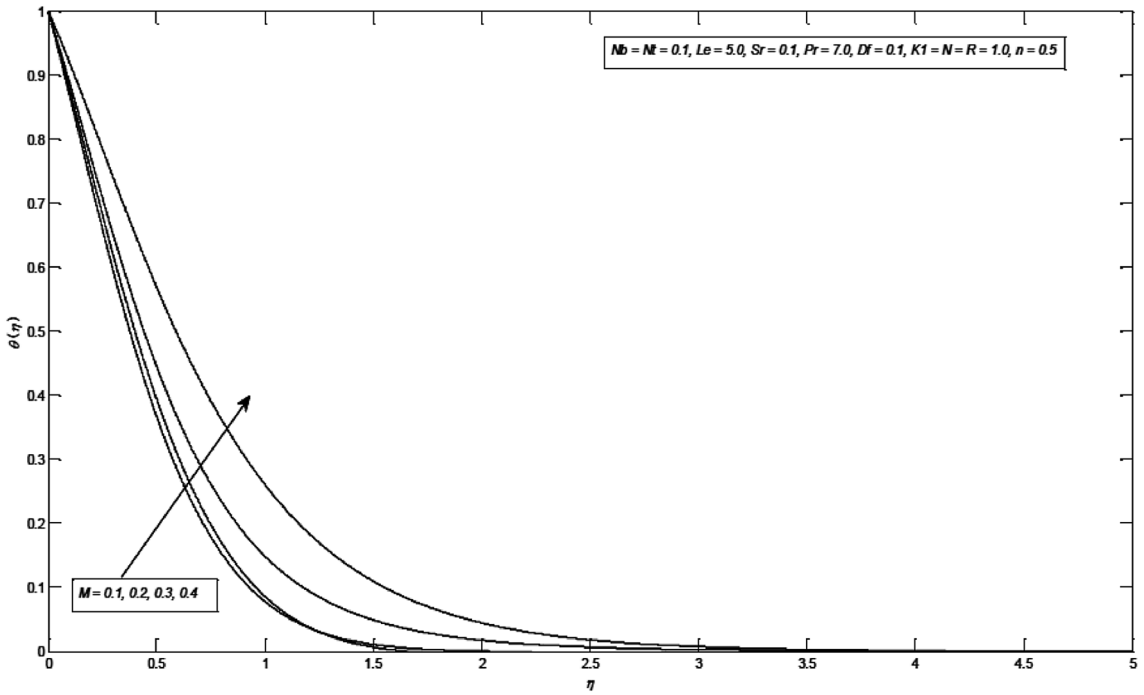

Fig. 10 The impacts of M on $\theta(\eta)$

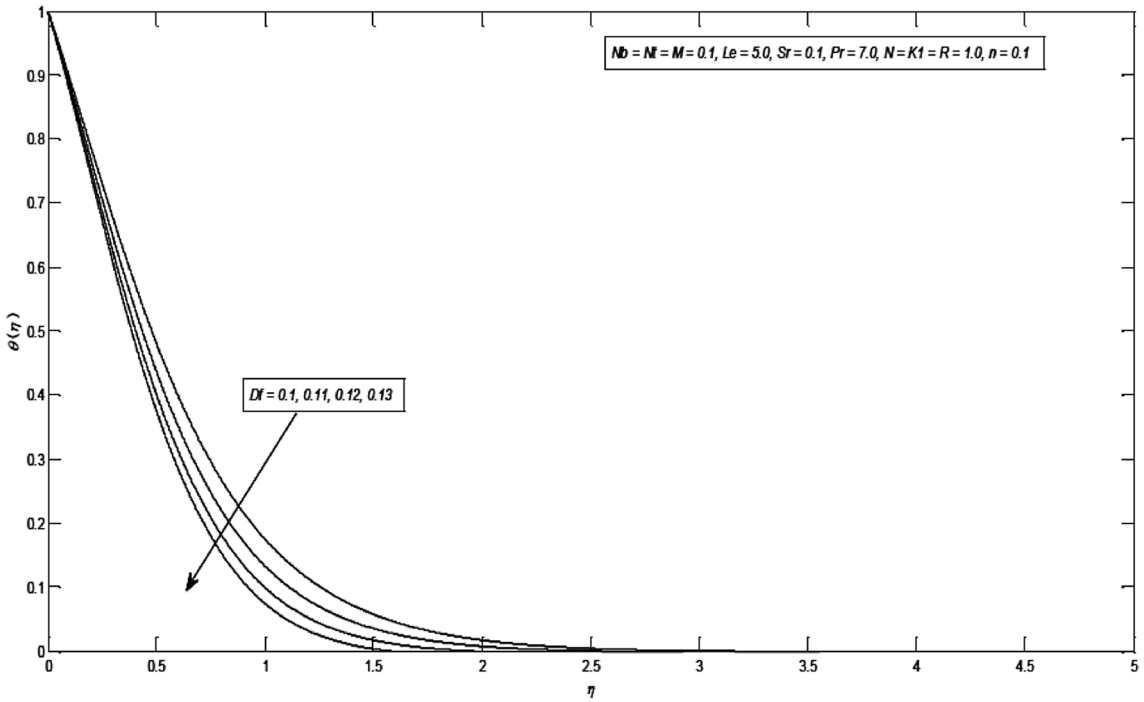

Fig. 11 The impacts of D_f on $\theta(\eta)$

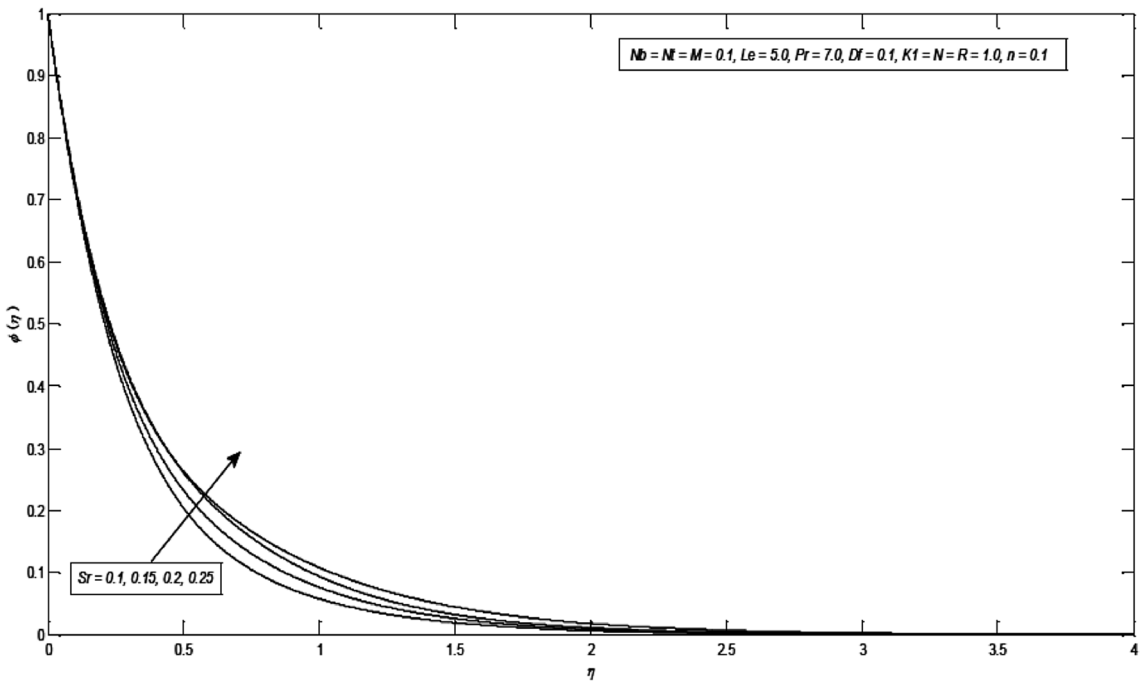

Fig. 12 The impacts of S_r on $\phi(\eta)$

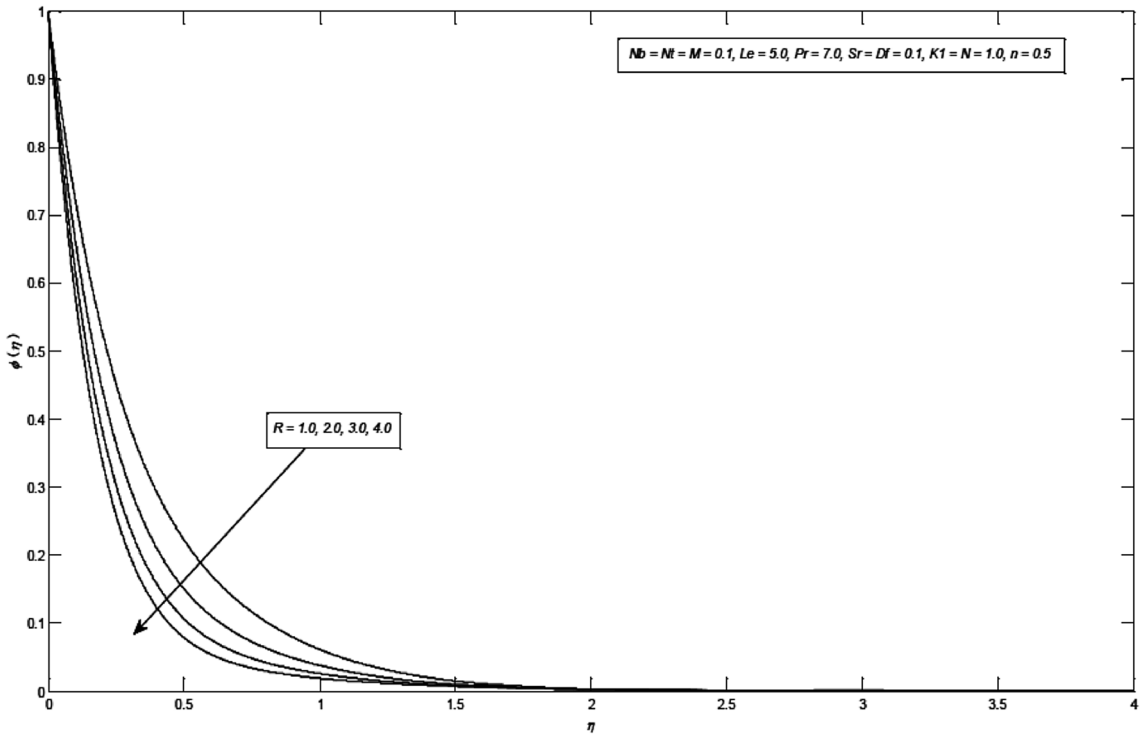

Fig. 13 The impacts of R on $\phi(\eta)$

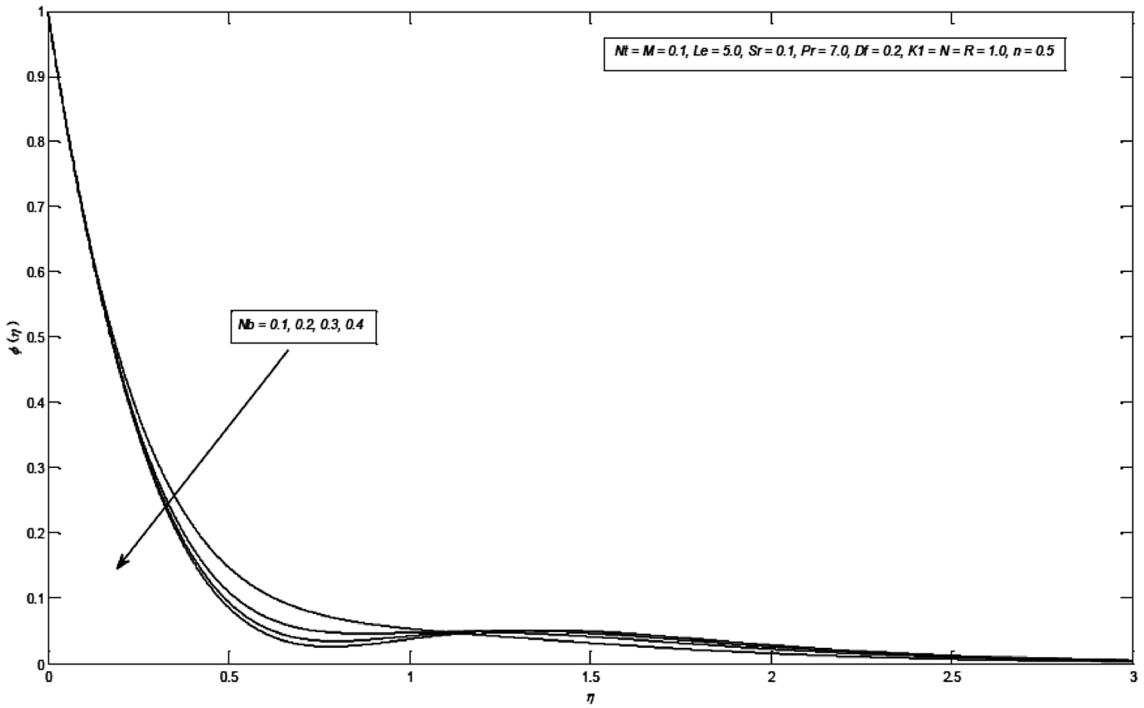

Fig. 14 The impacts of Nb on $\phi(\eta)$

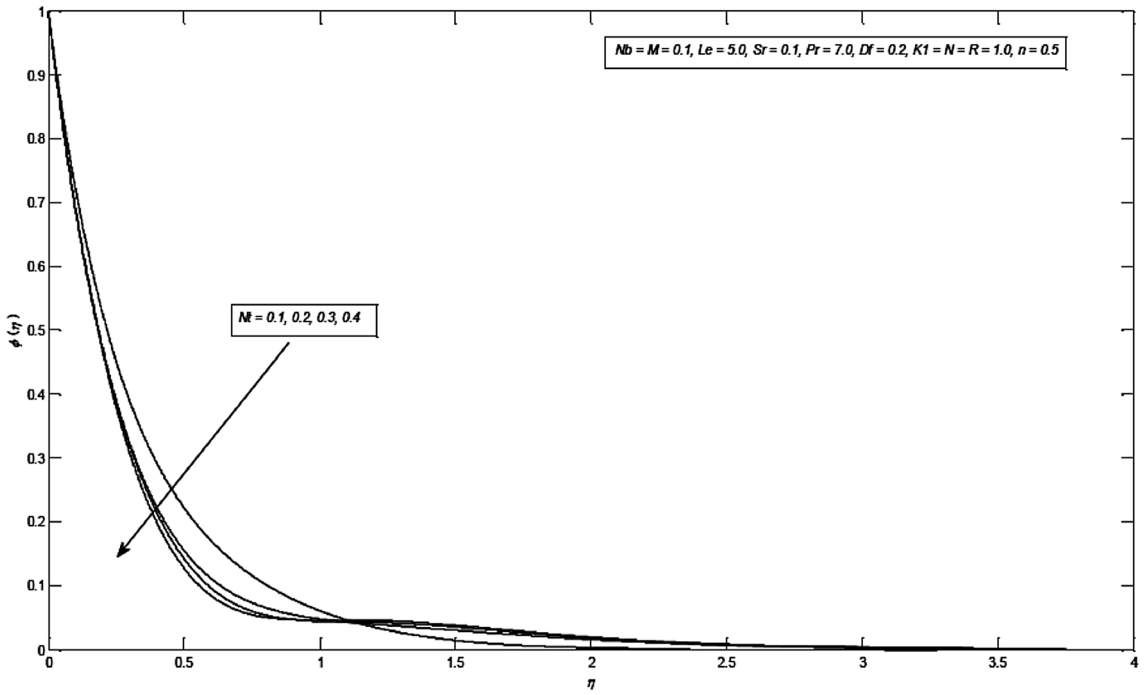

Fig. 15 The impacts of Nt on $\phi(\eta)$

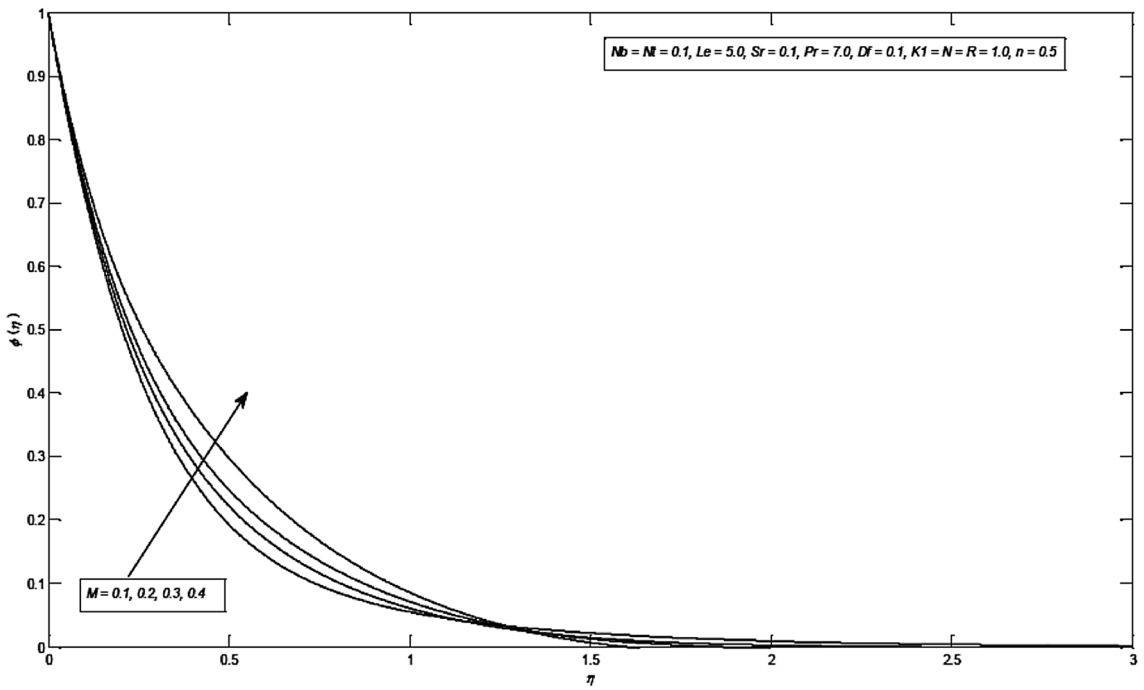

Fig. 16 The impacts of M on $\phi(\eta)$

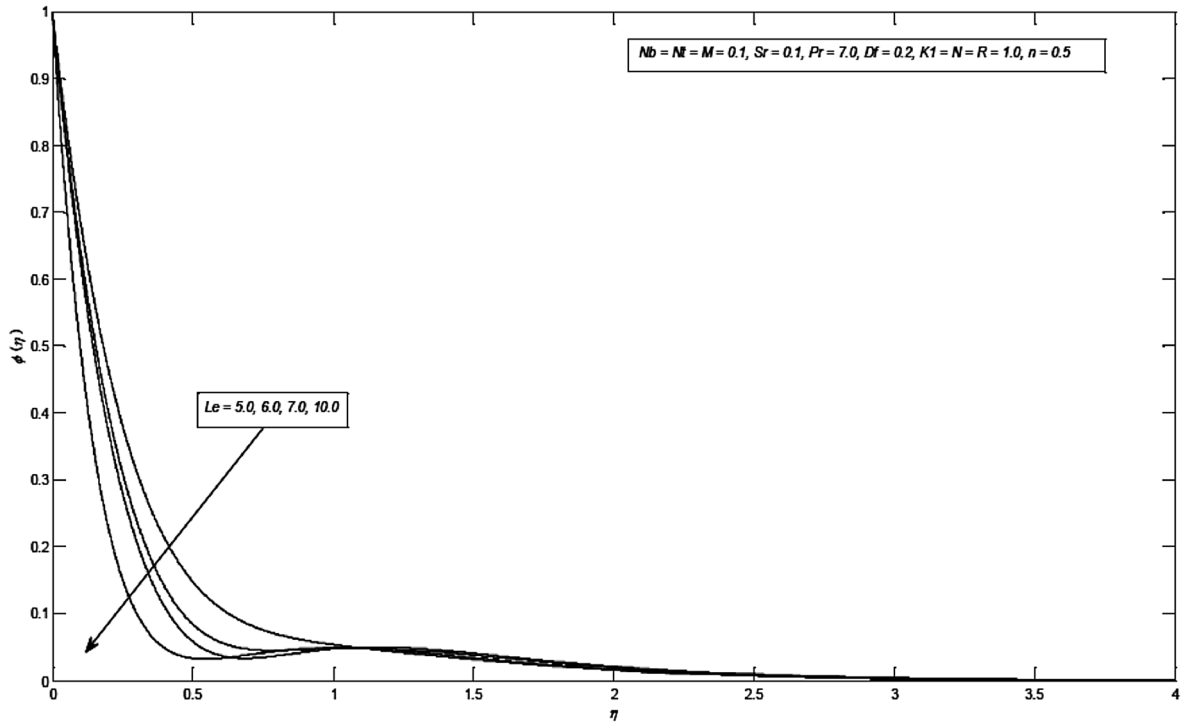

Fig. 17 The impacts of Le on $\phi(\eta)$

the values of M. Whereas this profile reduces in case of increasing the values of Le, which is depicted by Fig. 17.

4 Conclusions

The present study provides Soret–Dufours and thermal stratification effects on hydromagnetics nanofluid flow engendered by stretched surface in exponential manner inserted inside the porous medium. The transformation equations lead to transform the equations showing flow behavior of nanofluid into differential equations in ordinary form. Then the Keller box method is applied on resultant equations to get clear insight of governing parameters by numerical computations. Although, a number of studies are available in the literature on nanofluid flow with different geometries but in the light of growing applications of the nanofluids in industry and engineering. We considered the nanofluid along with Soret and Dufour impacts in the stratified porous medium. A couple of instances such as atomic surplus disposal, hydrology and thermal vigour are noteable. Results derived from this investigation can be summarized as

1. Increase of the magnetic parameter tends to enhance the temperature and concentration profiles as well.
2. Due to increase in Dufour parameters, temperature profile reduces. On contrast, larger the Soret parameter results increase in concentration profile.
3. Radiative and chemical reactive constraints show converse behaviour on temperature profile. The temperature profile increases in relation with enhancement of chemical reaction parameter whereas this profile displays reduction by rising radiation parameter.
4. The temperature profile decreases by rising the Prandlt number whereas the concentration profile declines by enhancing the Lewis number.
5. The temperature profile enhances by increasing both parameters signifying Brownian motion and thermophoresis effects whereas concentration profile expresses reverse behaviour in case of these parameters.

Compliance with ethical standards

Conflict of interest The authors declare that they have no conflict of interest.

References

1. Eckert ER (1972) Analysis of heat and mass transfer (No 04 QC320 E2)
2. Chapman S, Cowling TG (1953) The mathematical theory of non-uniform gases. Cambridge Mathematical Library
3. Hirshfelder JO, Curtis CF, Bird RB (1954) Molecular theory of gases and liquids. Wiley, New York
4. Tsai R, Huang JS (2009) Numerical study of Soret and Dufour effects on heat and mass transfer from natural convection flow over a vertical porous medium with variable wall heat fluxes. Comput Mater Sci 47:23–30
5. Mahdy A (2010) Soret and Dufour effect on double diffusion mixed convection from a vertical surface in a porous medium saturated with a non-Newtonian fluid. J Non-Newtonian Fluid Mech 165:568–575
6. Chamkha AJ, Ben-Nakhi A (2008) MHD mixed convection-radiation interaction along a permeable surface immersed in a porous medium in the presence of Soret and Dufour's Effects. Heat Mass Transf 44:845
7. Tai BC, Char MI (2010) Soret and Dufour effects on free convection flow of non-Newtonian fluids along a vertical plate embedded in a porous medium with thermal radiation. Int Commun Heat Mass Transf 37:480–483
8. Dzulkifli NF, Bachok N, Pop I, Yacob NA, Arifin NM, Rosali H (2017) Soret and Dufour effects on unsteady boundary layer flow and heat transfer of nanofluid over a stretching/shrinking sheet: a stability analysis. J Chem Eng Process Technol 8:1000336
9. Hayat T, Nasir T, Khan MI, Alsaedi A (2018) Numerical investigation of MHD flow with Soret and Dufour effect. Results Phys 8:1017–1022
10. Besthapu P, Haq RU, Bandari S, Al-Mdallal QM (2017) Mixed convection flow of thermally stratified MHD nanofluid over an exponentially stretching surface with viscous dissipation effect. J Taiwan Inst Chem Eng 71:307–314
11. Devi SPA, Kandasamy R (2003) Effects of chemical reaction, heat and mass transfer on non-linear MHD flow over an accelerating surface with heat source and thermal stratification in the presence of suction or injection. Commun Numer Methods Eng 19:513–520
12. Hayat T, Shehzad SA, Al-Sulami HH, Asghar S (2013) Influence of thermal stratification on the radiative flow of Maxwell fluid. J Braz Soc Mech Sci Eng 35:381–389
13. Hayat T, Waqas M, Shehzad SA, Alsaedi A (2016) On 2D stratified flow of an Oldroyd-B fluid with chemical reaction: an application of non-Fourier heat flux theory. J Mol Liq 223:566–571
14. Choi SUS, Eastman JA (1995) Enhancing thermal conductivity of fluids with nanoparticles. In: Conference: 1995 International mechanical engineering congress and exhibition, San Francisco, CA (United States), 12–17 Nov 1995
15. Chaurasia P, Kumar A, Yadav A, Rai PK, Kumar V, Prasad L (2019) Heat transfer augmentation in automobile radiator using Al_2O_3-water based nanofluid. SN Appl Sci 1:257
16. Shiriny A, Bayareh M, Nadooshan AA (2019) Nanofluid flow in a microchannel with inclined cross-flow injection. SN Appl Sci 1:1015
17. Latha D, Prabu P, Gnanamoorthy G, Munusamy S, Sampurnam S, Arulvasu C, Narayanan V (2019) Size-dependent catalytic property of gold nanoparticle mediated by Justicia adhatoda leaf extract. SN Appl Sci 1:134
18. Chen X, Lei J, Wang Y, Zhu W, Yao W, Duan T (2019) Ternary Ag nanoparticles/natural-magnetic SiO 2-nanowires/reduced graphene oxide nanocomposites with highly visible photocatalytic activity for 4-nitrophenol reduction. SN Appl Sci 1:130
19. Tiwari RK, Das MK (2007) Heat transfer augmentation in a two-sided lid-driven differentially heated square cavity utilizing nanofluids. Int J Heat Mass Transf 50:2002–2018
20. Buongiorno J (2006) Convective transport in nanofluids. J Heat Transf Trans ASME 128:240–250
21. Sheikholeslami M, Rokni HB (2018) Magnetic nanofluid flow and convective heat transfer in a porous cavity considering Brownian motion effects. Phys Fluids 30:012003
22. Sheikholeslami M, Sheremet MA, Shafee A, Li Z (2019) CVFEM approach for EHD flow of nanofluid through porous medium within a wavy chamber under the impacts of radiation and moving walls. J Therm Anal Calorim 138:573–581
23. Sheikholeslami M (2018) Influence of magnetic field on Al_2O_3-H_2O nanofluid forced convection heat transfer in a porous lid driven cavity with hot sphere obstacle by means of LBM. J Mol Liq 263:472–488
24. Waqas H, Khan SU, Shehzad SA, Imran M (2019) Radiative flow of Maxwell nanofluid containing gyrotactic microorganism and energy activation with convective Nield conditions. Heat Transf Asian Res 48:1663–1687
25. Waqas M, Shehzad SA, Hayat T, Khan MI, Alsaedi A (2019) Simulation of magnetohydrodynamics and radiative heat transport in convectively heated stratified flow of Jeffrey nanofluid. J Phys Chem Solids 133:45–51
26. Rauf A, Abbas Z, Shehzad SA (2019) Interactions of active and passive control of nanoparticles on radiative magnetohydrodynamics flow of nanofluid over oscillatory rotating disk in porous medium. J Nanofluids 8:1385–1396
27. Li J, Liu L, Zheng L, Bin-Mohsin B (2016) Unsteady MHD flow and radiation heat transfer of nanofluid in a finite thin film with heat generation and thermophoresis. J Taiwan Inst Chem Eng 67:226–234
28. Mahanthesh B, Gireesha BJ, Shehzad SA, Rauf A, Kumar PS (2018) Nonlinear radiated MHD flow of nanoliquids due to a rotating disk with irregular heat source and heat flux condition. Phys B Condens Matter 537:98–104
29. Sheikholeslami M (2019) Numerical approach for MHD Al_2O_3–water nanofluid transportation inside a permeable medium using innovative computer method. Comput Methods Appl Mech Eng 344:306–318
30. Sheikholeslami M, Mehryan SAM, Shafee A, Sheremet MA (2019) Variable magnetic forces impact on magnetizable hybrid nanofluid heat transfer through a circular cavity. J Mol Liq 277:388–396
31. Sheikholeslami M (2019) New computational approach for exergy and entropy analysis of nanofluid under the impact of Lorentz force through a porous media. Comput Methods Appl Mech Eng 344:319–333
32. Sheikholeslami M, Shafee A, Zareei A, Haq R, Li Z (2019) Heat transfer of magnetic nanoparticles through porous media including exergy analysis. J Mol Liq 279:719–732
33. Sheikholeslami M, Shehzad SA, Abbasi FM, Li Z (2018) Nanofluid flow and forced convection heat transfer due to Lorentz forces in a porous lid driven cubic enclosure with hot obstacle. Comput Methods Appl Mech Eng 338:491–505
34. Hosseini SR, Ghasemian M, Sheikholeslami M, Shafee A, Li Z (2019) Entropy analysis of nanofluid convection in a heated porous microchannel under MHD field considering solid heat generation. Powder Tech 344:914–925
35. Sajjadi H, Delouei AA, Sheikholeslami M, Atashafrooz M, Succi S (2019) Simulation of three dimensional MHD natural convection using double MRT Lattice Boltzmann method. Phys A Stat Mech Appl 515:474–496
36. Shafee A, Haq RU, Sheikholeslami M, Herki JAA, Nguyen TK (2019) An entropy generation analysis for MHD water based

Fe3O4 ferrofluid through a porous semi annulus cavity via CVFEM. Int Commun Heat Mass Transf 108:104295
37. Anwar MI, Kasim ARM, Ismail Z, Salleh MZ, Shafie S (2013) Chemical reaction and uniform heat generation or absorption effects on MHD stagnation-point flow of a nanofluid over a porous sheet. World Appl Sci J 24:1390–1398
38. Shateyi S, Motsa SS, Sibanda P (2010) The effects of thermal radiation, Hall currents, Soret, and Dufour on MHD flow by mixed convection over a vertical surface in porous media. Math Probl Eng 2010:627475
39. Pal D, Mondal H (2011) Effects of Soret Dufour, chemical reaction and thermal radiation on MHD non-Darcy unsteady mixed convective heat and mass transfer over a stretching sheet. Commun Nonlinear Sci Numer Simul 16:1942–1958
40. Rafique K, Anwar MI, Misiran M (2019) Keller-box study on Casson nano fluid flow over a slanted permeable surface with chemical reaction. Asian Res J Math 14:1–17
41. Chen CH (2008) Effects of magnetic field and suction/injection on convection heat transfer of non-Newtonian power-law fluids past a power-law stretched sheet with surface heat flux. Int J Thermal Sci 47:954–961
42. Cess RD (1966) The interaction of thermal radiation with free convection heat transfer. Int J Heat Mass Transf 9:1269–1277
43. Cebeci T, Bradshaw P (1984) Physical and computational aspects of convective heat transfer. Springer, New York
44. Bidin B, Nazar R (2009) Numerical solution of the boundary layer flow over an exponentially stretching sheet with thermal radiation. Eur J Sci Res 33:710–717